Characteristics of aerosol types and identifying the external dust sources (the case of Mashhad city, Iran)

Alireza Rashki[1*], *Somayeh* Feizollahi[1], and *Ali* Bayat[2]

[1]Department of Desert and Arid Zones Management, Ferdowsi University of Mashhad, Mashhad, Iran
[2]Faculty of Science, Zanjan University, Zanjan, Iran

Abstract. Aerosols, consisting of solid, liquid, and gaseous particles, emerge from both natural and human-induced origins, impacting air quality over substantial distances. This investigation focuses on discerning dust origins in the polluted city of Mashhad, Iran. Crucial parameters, such as aerosol optical thickness (AOT) and Ångström exponent (AE), play a vital role in understanding aerosols and atmospheric pollutants. Ground-based sun photometers (Calitoo) were employed for calculating AOT and AE at different wavelengths to determine the aerosol characteristics and to reveal the prevalence of urban-industrial pollution. The research detect dust and identifies dust sources from both domestic and neighboring deserts, noting seasonal variations. The results highlight the importance of comprehensive monitoring and understanding of aerosol dynamics for effective air quality management.

1 Introduction

Aerosols, comprising solid, liquid, and gaseous particles suspended in the air, are derived from both natural and human-induced sources. These particles, whether originating naturally or through human activities, can traverse significant distances, impacting air quality [1]. Positioned in the global dust belt and the Middle East, Iran faces diverse sources of dust both domestically and from neighbouring countries, contributing to critical air pollution concerns for urban and rural populations. The repercussions of air pollution extend to both human health and the environment, necessitating comprehensive investigations.

Parameters such as aerosol optical thickness (AOT) and Ångström exponent (AE) are essential tools for studying aerosols and atmospheric pollutants. AOT, a dimensionless metric, evaluates light transmission through the atmosphere, reflecting aerosol-induced absorption and scattering. Simultaneously, AE characterizes atmospheric particle dimensions by comparing aerosol optical thickness across different wavelengths. These metrics provide valuable insights into discerning between natural and anthropogenic aerosol types [2].

The assessment of air quality relies on changes in direct sunlight intensity, quantifiable through optical thickness. AOT values serve as indicators of aerosol concentration, with lower values signifying cleaner air and higher values indicating heightened aerosol concentration, contributing to increased air pollution and reduced horizontal visibility. Ground-based solar spectrometers, such as the Calitoo sun photometer employed in this research, enable the calculation of aerosol optical thickness across various wavelengths.

Numerous studies, including those by [1-4], have contributed valuable insights into aerosol characteristics in diverse geographic locations. Employing various methodologies and instruments such as handheld sun-photometers and satellite data, these investigations collectively enhance our understanding of aerosol dynamics and their implications for air quality.

2 Methods and materials

2.1 Mashhad City and sun-photometer measurements

Mashhad is as one of the most polluted cities in Iran. Atmospheric pollutants (small-sized) and dust aerosols (large-sized) prevail, significantly influencing air pollution levels. The identification of pollutant types and their distribution is crucial for developing strategies to mitigate this problem. The primary pollutants contributing to the deterioration of air quality in the city are suspended particles. One source of these particles is desert dust originating from nearby deserts, such as the Central Iran Desert and the deserts of Turkmenistan. Sun photometer data can specify the types of elements and the extent of pollutant contributions. To achieve this, two measurement stations equipped with Calitoo handheld sun photometers were established. The initial station is situated within the city at Ferdowsi University of Mashhad (FUM), while the second station, representing a suburban area, is located 1.5 km east of Mashhad city in Shahid Shushtari (SH) (Fig. 1). These stations aim to provide valuable information to comprehend and tackle air quality challenges in Mashhad.

* Corresponding author: a.rashki@um.ac.ir

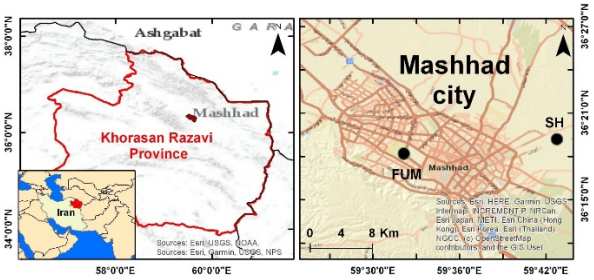

Fig. 1. The study area and location of measurement stations (SH&FUM).

The Calitoo sun-photometer (www.calitoo.fr), is a portable device measuring aerosol optical thickness at three wavelengths (465, 540, and 619 nm). It also computes the Ångström exponent, indicating particle size, using data from 465 nm and 619 nm. Sampling began at the SH station in January 2021 and at the FUM station in September 2021, continuing until December 2022 for both locations. The SH station had a sampling duration of 2 years, while the University station covered 1 year and 4 months. Sampling occurred on all days, excluding those with cloudy conditions that could affect solar radiation intensity and lead to potential errors. In total, there were 583 sampling days at the SH station and 279 days at the Ferdowsi University station. Each sampling session included a minimum of three or four repetitions. The level one data recorded at the SH station was 8753, and at the FUM station, it was 6984. Days with only one sampling session were excluded, removing 132 days for the SH station and 199 days for the University station due to cloudy conditions and singular data recording. Additional and erroneous data from level one recordings with the Calitoo sun-photometer were eliminated using its software, resulting in the conversion of the remaining original data to level 1.5 data. The SH had 1996 data points in level 1.5, and the Ferdowsi University station had 1549.

2.2 Aerosol classification

Aerosols are categorized through various methods, and one of the most effective approaches involves using Aerosols Optical Thickness (AOT) and Ångström exponent (AE) values. AOT measures the density of aerosol particles in the atmosphere, while AE serves as a metric for the dimensions and size of these particles. Since aerosols exhibit diverse characteristics and dimensions, employing both AOT and AE values allows for a comprehensive classification based on size.

Airborne pollutants include dust, urban-industrial pollution, biomass particles, and sea salt (marine aerosols). These pollutants differ in particle sizes, chemical compositions, carbonaceous aerosol fractions, inorganic species, and heavy metals. These characteristics determine the physical, chemical, and optical properties of aerosols, influencing their impact on climate [5,7]. In the city of Mashhad, prevailing atmospheric conditions, influenced by its unique geographical location and distance from seas and extensive forests, mainly consist of dust and urban-industrial pollution, with atmospheric mixing of these primary aerosol types. The identification of cleaner air conditions can also be achieved through the analysis of AOT and AE values. Table 1 provides essential threshold values for determining aerosol types, as illustrated in Fig. 2. This classification system matrix divides aerosols into five distinct groups: dust, urban-industrial pollution, mixed aerosols combining urban pollution and dust (contaminated dust), and clear air. Aerosols that do not fall into any of these categories are labelled as undefined. Figure 2 depicts the classification of aerosols for the SH station and the FUM station, with the horizontal axis representing AOT values and the vertical axis indicating AE.

Table 1. Classification of aerosol types based on AOT and AE values.

Type	AOT	AE
Dust	>0.3	<0.7
Urban	>0.2	>0.7
Clear	<0.1	any
Mixed	otherwise	otherwise

2.3 Dust backward trajectories

HYSPLIT, which stands for Hybrid Single Particle Lagrangian Integrated Trajectory, is a widely used atmospheric transport and dispersion model. It is employed to simulate the movement of air masses and the dispersion of various substances, including pollutants, particulate matter, or dust particles, over time [8].

HYSPLIT trajectories refer to the paths that air parcels or particles take as they move through the atmosphere. Researchers and environmental scientists use HYSPLIT Trajectories to understand the spatial distribution and movement patterns of airborne substances, such as dust. By analysing these trajectories, one can gain insights into the potential sources, pathways, and destinations of atmospheric particles, aiding in the assessment of air quality and the study of long-range transport phenomena [9]. To detect the source regions of Mashhad dust, 40 h backward trajectories of air masses arriving at the Mashhad city on the dusty days which were detected from Calitoo data, were determined using Hybrid Single Particle Lagrangian Integrated Trajectory model version 4 (HYSPLIT 4).

2.4 Identifying of dust sources

During periods of dust events and along the predetermined dust trajectories, we obtained daily images from the Terra and Aqua satellites' MODIS (MODerate-resolution Imaging Spectroradiometer) sensors (two images per day). To discern and measure dust sources, an enhanced Brightness Dust Index (eBDI) was utilized as a dust density index [10]. Furthermore, hourly satellite composite data from the Meteosat Second Generation (MSG) and Spinning Enhanced Visible and Infra-Red Imager (SEVIRI) was used to pinpoint regions of dust dispersion [11] impacting Mashhad City. The dust product is an RGB (Red, Green, Blue) composite based upon infrared channel data from the Meteosat Second Generation satellite. It is designed

to monitor the evolution of dust storms during both day and night.

3 Results and discussion

3.1 Type of aerosols in Mashhad City

At the SH station, 56% of the data falls into the category of urban-industrial pollution, 29% in the category of mixed dust-laden air, and 13% in category of dust. 5.1% of the data is undefined and only 2.0% represents clean air. In this station, urban-industrial pollutants dominate, followed by mixed data and then dust data.

At FUM station, 67% of the data is categorized as urban-industrial pollution, 15% as clean air, 6% as dust, and both mixed and undefined data each account for 5%. Urban-industrial pollutants are predominant at the FUM station, while the other categories have approximately equal proportions. It shows the most dust from outside city settled and cannot enter into the city centre.

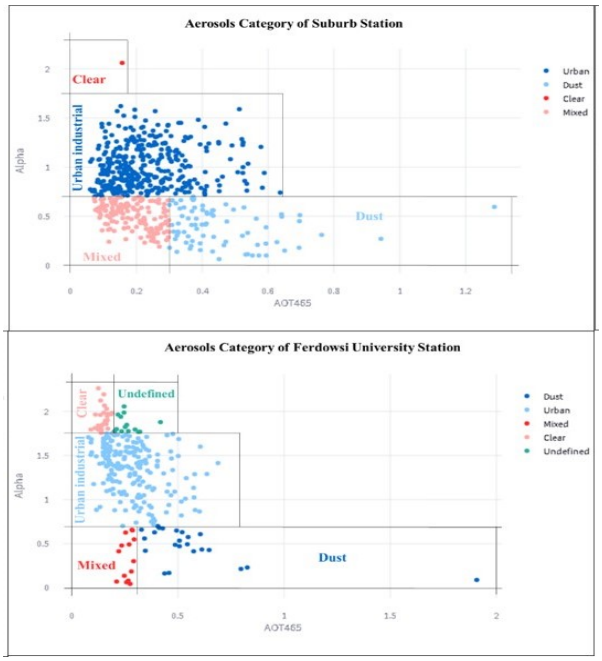

Fig. 2. Scatter plots of Ångström Exponent (AE, "Alpha") and Aerosol Optical Thickness (AOT) at 465 nm wavelength. The data points above panel represent measurements conducted at FUM, while down panel represent SH. Different colors are assigned to distinguish specific weather types, determined by the AOT and AE values' magnitudes.

3.2 Monthly and seasonal number of dust days

Changes over time reveal that Mashhad City experiences the highest frequency of dust events in March and April, with a subsequent decline in the following months. Notably, the summer season shows the highest dust levels, followed by spring, autumn, and winter, each exhibiting lower levels of dust (Fig. 3). Analysis of two monitoring stations indicates that airborne dust is more prominent on the outskirts of Mashhad City (Station SH) than in the city centre (Station FUM). This suggests that buildings may play a role in trapping dust particles in these areas.

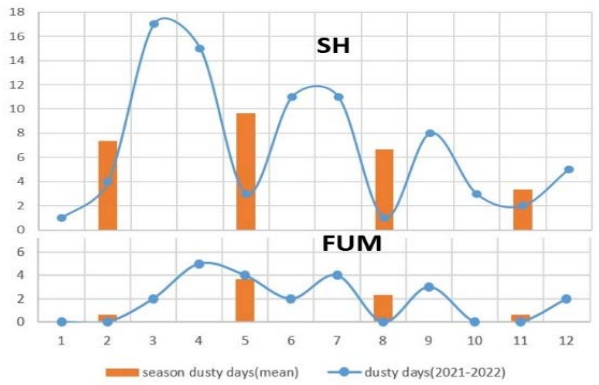

Fig. 3. Monthly and seasonal dusty days in two-measured stations.

3.3 HYSPLIT trajectories of dusty days

HYSPLIT backward trajectories were obtained for every day of dusty days of Mashhad city (2021–2022). The 40 h backward trajectories were obtained which show the origin and pathways of the air masses arriving at the Mashhad city at the specific observed dust time. Based on the score matrix of these trajectory data, two clusters were found that are named in this study by their origins and the entry direction to the study site. The backward trajectories of each of the two clusters are presented in Fig. 4 showing the ranges of horizontal coordinates representing each cluster. It shows in winter all dust comes from south west direction.

Hence, in the winter season, the domestic deserts of Iran and the deserts of Iraq, Syria, and Saudi Arabia can serve as potential origins for dust entering Mashhad. However, the dynamics change entirely during the summer season, where dust moves from the eastern region towards Mashhad. To put it differently, in the summer, the western deserts, including Sarakhs, Turkmenistan, and Uzbekistan, become potential sources of dust for Mashhad. In both the fall and spring seasons, dust typically approaches from both directions, with a greater prevalence from Iran's internal deserts in the fall and more dominance from Turkmenistan in the spring.

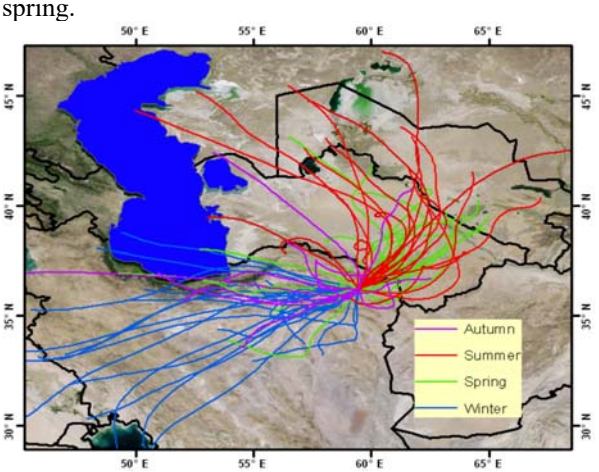

Fig. 4. The origins and pathways of 40 h HYSPLIT backward trajectories for dusty days in Mashhad city (2021–2022).

3.4 Origin of dust at Mashhad

The analysis focused on days with dust events and the two days preceding them, utilizing MODIS satellite images, hourly SEVIRI images, and the MODIS eBDI dust index (Fig. 5) along the trajectories. The findings revealed that 19% of the days showed no evidence of dust along the trajectory paths, indicating localized dust, possibly generated by human activities within the city or its vicinity. On 81% of the dusty days in Mashhad, the dust originated from desert areas, particularly during the winter and late autumn, with a higher contribution from western deserts such as Nishabour, Gonabad, Bajestan, and the central deserts of Iran. Instances were noted where dust with origins in Iraq and Syria reached Mashhad. In the summer and late spring, dust typically originated from the internal deserts of Sarakhs and the countries of Turkmenistan and Uzbekistan, with a predominant contribution from the Qaraqum Desert. Less dust reached Mashhad from the Aral Sea region during this period. In spring and autumn, dust commonly arrived from both western and eastern directions. The approximately one-day travel time for desert dust to reach Mashhad allows for predictive monitoring of dust events in the city by observing these source areas.

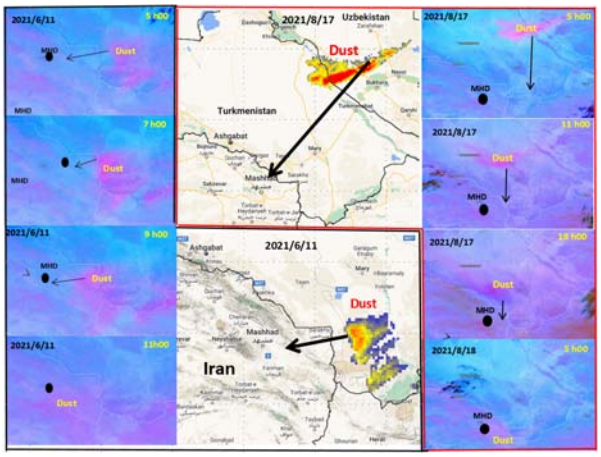

Fig. 5. Source of dust arriving to Mashhad on 11 June 2021 (left panel) and 17 August 2021 (right panel). Right and left images show the hourly SEVIRI images (pink colors are dust) and eBDI from MODIS in the centre panel.

4 Conclusion

This study delved into the intricacies of aerosols and air quality in Mashhad City, Iran, with a specific focus on discerning the sources and characteristics of airborne particles. For this purpose, measurements were conducted using Calitoo sun photometers at two stations, aiming to classify aerosols based on AOT and AE values. The resulting classification matrix distinguished between dust, urban-industrial pollution, mixed aerosols, and clean air. HYSPLIT trajectories were utilized to trace the movement of air masses and pinpoint potential dust sources. Additionally, the study harnessed MODIS and SEVIRI satellite data to detect dust. Results and discussions yielded insights into the prevailing aerosol types in Mashhad, with urban-industrial pollution taking the lead. Examination of the seasonality of dusty days revealed heightened occurrences in March and April, reaching a peak during the summer season. HYSPLIT trajectories underscored distinct dust sources in winter and summer, highlighting the influence of domestic deserts and neighboring countries. The origin of Mashhad dust was systematically traced using backward trajectories, revealing contributions from various desert areas with seasonal variations in predominant sources.

References

1. J.F. Léon, A.B. Akpo, M. Bedou, J. Djossou, M. Bodjrenou, V. Yoboué, C. Liousse, Atmos. Chem. Phys. **21(3)**, 1815–1834, https://doi.org/10.5194/acp-21-1815-2021 (2021)
2. A. Bayat, A. Assarenayati, Atmos. Environ. **295**, 119570, https://doi.org/10.1016/j.atmosenv.2022.119570 (2023)
3. S.P. Acharya, A. Mukherjee, M.S. Janaki, Phys. Rev. E **104(1)**, 014214, https://doi.org/10.1103/PhysRevE.104.014214 (2021)
4. O.E. Obisesan, Int. J. Environ. Clim. **11(6)**, 150–161, https://doi.org/10.9734/ijecc/2021/v11i630431 (2021)
5. U.C. Dumka, S.D. Saheb, D.G. Kaskaoutis, Y. Kant, D. Mitra, Environ. Sci. Pollut. Res. **23**, 25467–25484, https://doi.org/10.1007/s11356-016-7766-y (2016)
6. P.N. Patel, U.C. Dumka, K.N. Babu, A.K. Mathur, Sci. Total Environ. **599–600**, 165–180, https://doi.org/10.1016/j.scitotenv.2017.04.168 (2017)
7. S. Romano, M.R. Perrone, G. Pavese, F. Esposito, M. Calvello, Atmos. Environ. **203**, 35–47, https://doi.org/10.1016/j.atmosenv.2019.01.037 (2019)
8. A. Aili, H. Xu, T. Kasim, A. Abulikemu, Atmosphere **12(1)**, 113, https://doi.org/10.3390/atmos12010113 (2021)
9. A. Alebić-Juretić, B. Mifka, J. Kuzmić, Sci. Total Environ. **912**, 169320, https://doi.org/10.1016/j.scitotenv.2023.169320 (2024)
10. L. Yang, L. She, Y. Che, X. He, C. Yang, Z. Feng, Appl. Sci. **13(3)**, 1365, https://doi.org/10.3390/app13031365 (2023)
11. O. Lavi Bekin, O. Crouvi, D.G. Blumberg, Remote Sens. **12(17)**, 2775, https://doi.org/10.3390/rs12172775 (2020)